Hindawi
International Journal of RF and Microwave Computer-Aided Engineering
Volume 2023, Article ID 1038325, 10 pages
https://doi.org/10.1155/2023/1038325

Research Article

Design of Novel Ultrabroadband Printed Antenna and Its Efficient Optimization Using Self-Adaptive Hybrid Differential Evolution Algorithm

Tian-Ye Gao, Yong-Chang Jiao, and Yi-Xuan Zhang

National Key Laboratory of Antennas and Microwave Technology, Xidian University, Xi'an, Shaanxi 710071, China

Correspondence should be addressed to Yong-Chang Jiao; ychjiao@xidian.edu.cn

Received 16 February 2023; Revised 10 May 2023; Accepted 15 May 2023; Published 1 June 2023

Academic Editor: Wen-Jun Lu

A novel compact ultra-broadband-modified fork-shaped printed antenna is optimized efficiently by using a self-adaptive hybrid differential evolution (SHDE) algorithm. Firstly, a novel compact ultra-broadband-modified fork-shaped printed antenna structure is proposed. The antenna with more compact size consists of a modified fork-shaped radiator and a modified ground plane, which can cover a very wide operating frequency band. The antenna is fed by a step-shaped microstrip line, and the modified ground plane consists of some rectangular slots and an L-shaped stub. Then, the SHDE algorithm is used to determine structural dimensions of the proposed antenna, and the antenna's performance is optimized while maintaining a cost-effective computation time. The optimized antenna with only 11.8 mm × 19.7 mm size covers -10 dB reflection coefficient bandwidth of 147.6% from 3.08 to 20.46 GHz. Finally, the antenna prototype is fabricated, and the measured results basically agree with the simulated ones. The proposed antenna can be viewed as an excellent candidate for realizing ultrabroadband transmission technology.

1. Introduction

For nearly two decades, ultrabroadband technology has attracted widespread attention for its applications in short-range wireless communications, imaging radar, remote sensing, and localization. To meet the requirements of more application scenarios, miniaturization and bandwidth broadening have become important research directions for ultrabroadband antennas. In order to significantly increase the bandwidth under the premise of ensuring small size, many design methods for the antennas were used such as L-shaped stubs [1–4], slits below the feed line [1–3, 5–10], and radiating patch slotting [2, 4, 6–9, 11–13]. By slotting and adding L-shaped stubs, the antenna proposed in Ref. [1] covers the frequency range of 3.1-10.6 GHz in a size of $15.8 \times 22\,\text{mm}^2$. By slotting under the feeder, the antenna proposed in Ref. [2] covers the frequency range of 2.6-13.04 GHz in a size of $25 \times 25\,\text{mm}^2$. By using slotted ground, tapered feeders, and U-shaped stubs, the antenna proposed in Ref. [6] covers the frequency range of 2.85-11.85 GHz in a size of $20 \times 28\,\text{mm}^2$. Besides, other methods have been implemented to enhance the impedance bandwidth [5, 14–16]. In Ref. [5], multiple rectangular notches are slotted on the ground and the patch, making the antenna structure look like a ladder. As a result, the antenna covers the frequency range of 2.96-19.4 GHz in a size of $30 \times 26\,\text{mm}^2$. In Ref. [14], a rectangular strip is connected to the circular patch to modify its shape, and a gap similar to the patch is slotted into the ground below the patch, making the antenna cover the frequency range of 2.97-11.32 GHz in a size of 19 $\times 24\,\text{mm}^2$. A fork-shaped patch, which is used in the antenna exhibited in Ref. [15], covers the frequency range of 2.3-2.5 GHz and 3.1-12GHz in a size of $42 \times 24\,\text{mm}^2$. In Ref. [16], by inserting an equilateral triangular slot into the ground plane, a much wider impedance bandwidth is realized in a size of $28 \times 24\,\text{mm}^2$. With the development of communication equipment, traditional ultrawideband (UWB) antennas covering the UWB frequency band of 3.1-10.6 GHz [17] only can no longer meet the requirements of increasing channel capacities, and the antenna frequency

band needs to be further broadened. Additionally, antennas with large sizes are not conducive to use. Thus, the ultrabroadband antennas covering wider frequency band than the UWB should be further miniaturized, and efficient optimization design of these ultrabroadband antennas is necessary and urgent.

Although several novel antennas have been proposed, how to determine their best structural parameter values to make the antennas achieve optimal performance remains a highly challenging task. Generally, parametric analyses are used to determine their structural parameter values, but the obtained parameter values are not globally optimal, since the interaction between these parameters is not considered. Local optimization algorithms, such as the quasi-Newton method as well as the Nelder and Mead simplex method, can yield satisfactory results. However, when complexity of the antenna structure increases, choosing a suitable initial value close to the global optimal solution in advance is very difficult, which may result in poor antenna performance. To address this issue, global optimization algorithms such as the differential evolution (DE) algorithm are commonly used for efficiently optimizing global performances of the antennas.

In order to improve the antenna structure so that its frequency band can be expanded as wide as possible under the premise of ensuring small size and global solution, it is particularly important to select an appropriate optimization algorithm. Since such antennas with many variables are difficult to design, global optimization algorithms are suggested to optimize the antenna structure. Among them, the DE has become a popular choice for many people to optimize the UWB antennas due to its easy use, strong robustness, and powerful global search capabilities [18–20]. In Ref. [21], the DE algorithm was used to realize the global optimization of a Yagi antenna. An efficient global optimization method based on the DE algorithm was proposed in Ref. [22], and an array antenna was successfully optimized to achieve better performance. In Ref. [23], the combination of DE and moment method was used to design a low-RCS antenna in a very short optimization time, which proved excellent global optimization performance of the DE algorithm. However, because the DE algorithm is essentially a random optimization algorithm based on the random search, it needs large amount of calculations and has the disadvantages of slow convergence speed. In addition, for different antenna problems, it is very difficult to set the control parameters reasonably for the DE algorithm, and the unreasonable setting of the control parameters will even greatly slow down the optimization process and deteriorate the quality of solutions.

In order to solve the above-mentioned problem that it is difficult to balance the miniaturization size and the wide frequency band, firstly, we propose a novel compact ultrabroadband printed antenna in this paper. L-shaped branch ground, slotting under the feeder, radiator slotting, and chamfering are used in the structural design, and the antenna bandwidth is further widened to cover as many frequencies as possible, under the premise of ensuring the antenna miniaturization. In addition to covering the UWB, the antenna also covers the X-band (8-12 GHz) [24] and Ku-band (12-18 GHz) [24], significantly increasing the application range. Then, in order to solve the problem that the DE algorithm takes too much time for multivariable optimization problems and its parameters are difficult to select, the optimization performance of three algorithms is compared and analyzed by using five benchmark problems. Simulation results indicate that suitable control parameters can be obtained by the SHDE algorithm without manual selection [25], and its final solutions have the highest qualities; thus, the SHDE algorithm is selected to optimize the antenna structure. Thanks to the improvement of antenna structure and the use of efficient global optimization algorithm, the final designed antenna in this paper features a small footprint of only 232.46 mm^2 with an operating band from 3.08 to 20.46 GHz ($|S_{11}| < -10$ dB). Compared with some existing antenna structures, the proposed structure can achieve a wider impedance bandwidth under smaller size constraints. The antenna structure is validated both numerically and experimentally. The measured reflection coefficients, gains, and radiation patterns are in basic agreement with the simulated ones.

2. Novel Compact Ultrabroadband Printed Antenna Structure

The geometry of the proposed antenna is shown in Figures 1 and 2. The microstrip feeder and the radiating patch in design A are improved, respectively, which are finally combined to obtain the proposed antenna. The shape of microstrip feeder is changed to make it a stepped structure, which significantly improves the impedance matching. The radiating patch has a plurality of rectangular slots, and its corners are cut to make the transition smooth. The final radiating patch is shaped like a modified fork. Through the above improvements, additional resonances are introduced, and the antenna impedance bandwidth is significantly increased. The impact of the above structural changes can be reflected in Figure 3. By improving the feeder structure, we can better achieve low-frequency impedance matching of the antenna, and by improving the radiating patch, high-frequency reflection coefficients of the antenna are greatly reduced. The combination of these two improvements achieves wider bandwidth characteristics of the proposed antenna.

The final proposed miniaturized antenna structure is shown in Figures 2 and 4. With the structural improvement process given in Figure 1, the proposed antenna achieves better performance while ensuring the compact size. More specifically, the design is implemented on a 0.756 mm thick Taconic RF-35 dielectric substrate ($\varepsilon_r = 3.5$, $\tan\delta = 0.0018$). The antenna comprises a modified fork-shaped radiator fed by a step-shaped microstrip line and a modified ground plane in the form of an L-shaped stub and a rectangular slit. All these improvements are to ensure widening the bandwidth under the premise of compact size. A comparison of the reflection coefficients of the above three models is shown in Figure 2, which reflects excellent performance of the combined improved design. The design vector with 25 variables is $x = (A, B, w_0, w_1, w_2, w_3, o_1, a_1, a_2, l_g, l_f, s_1, s_2, l_1, l_2, l_3, l_4,$

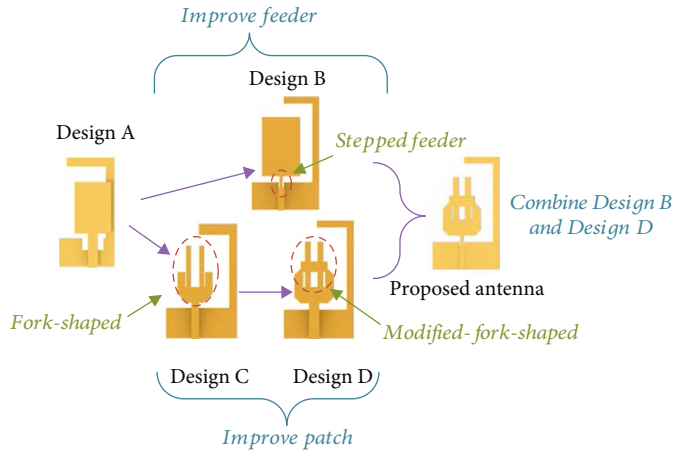

Figure 1: Design procedure of the proposed antenna.

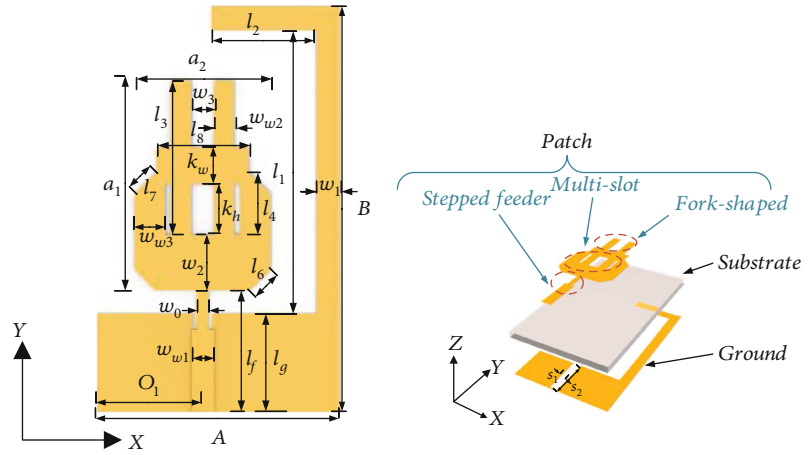

Figure 2: Structure of the proposed antenna: (a) top view and (b) 3D schematic.

$l_6, l_7, l_8, w_{w1}, w_{w2}, w_{w3}, k_h, k_w)^{\mathrm{T}}$. The slot at the ground and the entire patch are symmetrical about the A-O_1 axis, to ensure that the antenna achieves omnidirectional radiations as uniform as possible. The unit for all dimensions is millimeter. The calculation model of the antenna is implemented by Finite Integration Technology (FIT) in the CST microwave studio [26].

3. Optimization Design Procedure

Differential evolution (DE) is a heuristic random search algorithm based on group differences. The DE algorithm is a global optimization method formed by simulating genetic factors such as mutation, crossover, and selection in the process of biological genetics, as well as the evolution and development laws of natural species. People can use a number of parameters to control the combination of different individuals of the parent to generate new offspring. If the offspring are better than their parent, they will replace their parent. For the DE algorithm, the mutation, crossover, and selection operators are applied.

Suppose that $\mathbf{X} = (x_1, x_2, \cdots, x_D) \in S \subset R^D$ represents the vector to be optimized, $f(x)$ is the fitness function, $\mathbf{X}_{i,G} = (x_{1i,G}, x_{2i,G}, \cdots, x_{Di,G})$, $i = 1, 2, \cdots, NP$ are solution vectors in generation G, and NP is the population size. In the mutation operator, the mutation strategy DE/rand/1 is used to generate new solutions. For each $\mathbf{X}_{i,G}$, a mutation vector $\mathbf{V}_{i,G} = (v_{1i,G}, v_{2i,G}, \cdots, v_{Di,G})$ is produced according to

$$\mathbf{V}_{i,G} = \mathbf{X}_{r1,G} + F \cdot (\mathbf{X}_{r2,G} - \mathbf{X}_{r3,G}), \tag{1}$$

where $r1$, $r2$, and $r3$ are three different integers randomly selected from $\{1, 2, \ldots, NP\}$ such that $r1 \neq r2 \neq r3 \neq i$ and the scaling factor $F \in (0, 2]$ is a control parameter. In the crossover operator, the binomial crossover is used to produce a new trial vector $\mathbf{U}_{i,G} = (u_{1i,G}, u_{2i,G}, \cdots, u_{Di,G})$ according to

$$u_{ji,G} = \begin{cases} v_{ji,G}, & \text{if } \mathrm{rand}_j(0, 1) \leq \mathrm{CR} \text{ or } j = k \\ x_{ji,G}, & \text{otherwise} \end{cases}, \quad j = 1, 2, \cdots, D \tag{2}$$

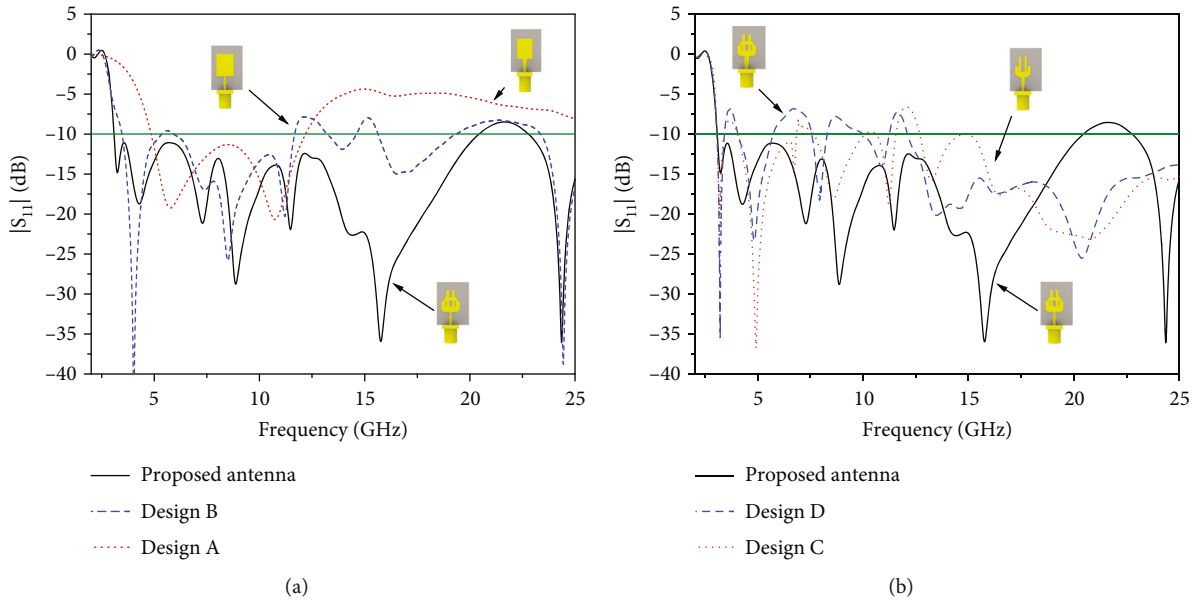

FIGURE 3: Simulated $|S_{11}|$ of five designs: (a) comparison of design A, design B, and the proposed antenna and (b) comparison of design C, design D, and the proposed antenna.

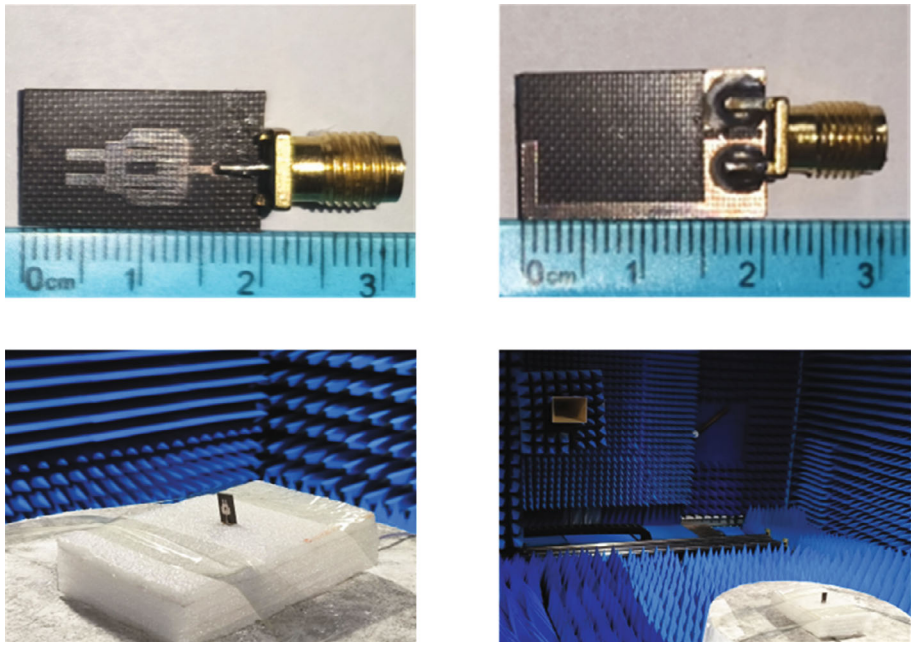

FIGURE 4: Photographs of the proposed antenna prototype and the measurement environment.

where the crossover rate $CR \in [0, 1]$ is another control parameter, k is an integer randomly chosen from $\{1, 2, \cdots, D\}$, and if $\text{rand}_j(0, 1)$ is the j-th evaluation of a uniform random number generator. In the selection operator, each offspring $\mathbf{U}_{i,G}$ competes with its parent $\mathbf{X}_{i,G}$ and survives only if its fitness value is better. Better individuals are selected to form the next-generation population, and the best individual $\mathbf{X}_{i,G}$ is recorded in each generation. The mutation, crossover, and selection operations are repeated until the stopping conditions are met.

In order to further significantly improve the local search ability of the DE algorithm, the simplified quadratic interpolation (SQI) with three individuals in the current population is added to the algorithm framework, and then, the hybrid DE (HDE) algorithm is implemented [27–29], in which the DE is used as a global optimizer and the SQI is served as a

local search operator. The calculation equations of the SQI operator used are expressed as follows:

$$A_{i,G} = \left(x_{2i,G}^2 - x_{3i,G}^2\right) f(\mathbf{X}_{1,G}) + \left(x_{3i,G}^2 - x_{1i,G}^2\right) f(\mathbf{X}_{2,G}) + \left(x_{1i,G}^2 - x_{2i,G}^2\right) f(\mathbf{X}_{3,G}), \quad (3)$$

$$B_{i,G} = (x_{2i,G} - x_{3i,G}) f(\mathbf{X}_{1,G}) + (x_{3i,G} - x_{1i,G}) f(\mathbf{X}_{2,G}) + (x_{1i,G} - x_{2i,G}) f(\mathbf{X}_{3,G}), \quad (4)$$

$$p_{i,G} = \frac{A_{i,G}}{2B_{i,G}}, \quad i = 1, 2, \cdots, D. \quad (5)$$

where $\mathbf{X}_{j,G} = (x_{j1,G}, x_{j2,G}, \cdots, x_{jD,G})$, $j = 1, 2, 3$, represent three individuals in the G-generation population and $\mathbf{P}_G = (p_{1,G}, p_{2,G}, \cdots, p_{D,G})$ is the obtained trial solution. The pseudocode of the SQI operator is listed as follows.

Step 0. Find the best and worst individuals $\mathbf{B}_G$ and $\mathbf{W}_G$ in the G-generation population and their fitness values f_b and f_w and set local iteration counter Local$K = 0$.

Step 1. While (Local$K \le$ Max$N$) do

Step 1.1. Randomly select two individuals $\mathbf{X}_{2,G}$ and $\mathbf{X}_{3,G}$ from the G-generation population such that $\mathbf{X}_{2,G} \ne \mathbf{X}_{3,G} \ne \mathbf{B}_G$ and set $\mathbf{X}_1 = \mathbf{B}_G$.

Step 1.2. Compute $\mathbf{P}_G = (p_{1.G}, p_{2,G}, \cdots, p_{D,G})$ by using Equation (5).

Step 1.3. Evaluate $f_p = f(\mathbf{P}_G)$ and set Local$K$ = Local $K + 1$.

Step 1.4. If $f_p \le f_w$, replace $\mathbf{W}_G$ by $\mathbf{P}_G$ in the G-generation population.

Verified by many numerical experiments, we suggest Max$N = 1$, if NP < 30; Max$N = 3$, otherwise. The SQI operator will greatly improve the local optimization ability of the DE algorithm.

Because both DE and HDE are particularly sensitive to the control parameters F and CR, different F and CR are suitable for different problems. Selecting suitable F and CR for the antenna design is a time-consuming and laborious work. In order to avoid manual selection of control parameters, the self-adaptive control method has been incorporated into the HDE algorithm to further improve antenna optimization performance [29, 30]. The control parameter setting scheme is used as follows:

$$F_{i,G+1} = \begin{cases} F_l + \text{rand}_1 \times F_u, & \text{if } \text{rand}_2 < 0.1, \\ F_{i,G}, & \text{otherwise}, \end{cases} \quad (6)$$

$$\text{CR}_{i,G+1} = \begin{cases} \text{rand}_3, & \text{if } \text{rand}_4 < 0.1, \\ \text{CR}_{i,G}, & \text{otherwise}, \end{cases} \quad (7)$$

where rand_j, $j = 1, 2, 3, 4$, are random numbers uniformly distributed from 0 to 1 and $F_l = 0.1$ and $Fu = 0.9$ are the lower and upper limits of F, respectively. Each individual in the G-generation population is set to the control parameters $F_{i,G}$ and $\text{CR}_{i,G}$ and retains $F_{i,G}$ and $\text{CR}_{i,G}$ of the winning individuals in the selection process to the $G + 1$ generation. In the optimization process, the contemporary global optimal individual parameters F_{Best} and CR_{Best} are selected as the optimal control parameters F and CR.

Execution process of the SHDE algorithm is shown as follows.

Step 1. Give the maximum number of generations ($G_{\max}$) or the number of function calls (NFC), and set $G = 0$.

Step 2. Generate the initial population with population size NP, and calculate the fitness function of each individual.

Step 3. Set $\text{rand}_2 = \text{rand}_4 = 0$, and calculate the control parameters $F_{i,0}$ and $\text{CR}_{i,0}$ according to Equation (7). Determine the best individual in the initial population, save its control parameters as $F_{\text{Best},0}$ and $\text{CR}_{\text{Best},0}$, and set $F = F_{\text{Best},0}$ and $\text{CR} = \text{CR}_{\text{Best},0}$.

Step 4. While ($G \le G_{\max}$ or other stopping criteria are not met)

Step 4.1. Mutation and crossover according to Equations (1) and (2). Invoke EM simulations to calculate the fitness results.

Step 4.2. Calculate the control parameters $F_{i,G+1}$ and C $\text{R}_{i,G+1}$ according to Equation (7).

Step 4.3. Selection according to the greedy strategy. The winning individual inherits the control parameters $F_{i,G+1}$ and $\text{CR}_{i,G+1}$.

Step 4.4. Retain the best individual in the G-generation population, save its control parameters as $F_{\text{Best},G}$ and C $\text{R}_{\text{Best},G}$, and set $F = F_{\text{Best},G}$ and $\text{CR} = \text{CR}_{\text{Best},G}$.

Step 4.5. Execute the SQI operator according to Equation (5).

Step 4.6. Set $G = G + 1$.

End while.

Step 5. Output the best solution.

Three algorithms, i.e., DE, HDE, and SHDE, are used to optimize the structure dimensions of the antenna in this paper. Six parameters w_{w2}, w_{w3}, k_h, k_w, l_7, and l_8, which have a greater impact on antenna performance and are difficult to determine, are selected as the optimization variables, and we set $x = (w_{w2}, w_{w3}, k_h, k_w, l_7, l_8)^T$. The maximum and minimum bounds for vector x are $x_{\min} = (0, 0, 1, 0.1, 0.1, 1)^T$ and $x_{\max} = (1.5, 2, 6, 3, 1, 8)^T$, respectively. Here, only the reflection coefficients $|S_{11}|$ in the frequency band are chosen as the optimization target. The fitness function is defined as

$$\text{fitness}(x) = \max_{1 \le i \le N_f} \left\{0, \text{RC}_{f_i}(x) + \alpha\right\}, \quad (8)$$

where $fi \in [fL, fH]$, $i = 1, 2, \cdots, N_f$, represent the sampling frequencies in the frequency band $[f_L, f_H]$ and N_f is the number of sampling points in the frequency band. In this

work, the equidistant frequencies are sampled, and the sampling interval is 0.023 GHz. In Equation (8), $\mathrm{RC}_{f_i}(\cdot)$ represents the modulus value of reflection coefficient of the antenna at frequency f_i with unit decibel. Our design target is $|S_{11}| < -10$ dB in the operating frequency band $[f_L, f_H]$. To achieve this goal, we choose $\alpha = 15$. For the compact printed antenna structure, we set $f_L = 3.1$ GHz and $f_H = 20$ GHz.

Five benchmark problems are also used to evaluate the optimization performance of three algorithms, i.e., DE, HDE, and SHDE, which are listed as follows.

Problem 1 (sphere model ($D = 10$)).

$$f(x) = \sum_{i=1}^{D} x_i^2, x_i \in [-100, 100], \quad i = 1, 2, \cdots, D. \tag{9}$$

Problem 2 (quartic function, i.e., noise ($D = 20$)).

$$f(x) = \sum_{i=1}^{D} i x_i^2 + \mathrm{random}[0, 1), \quad x_i \in [-1.28, 1.28], i = 1, 2, \cdots, D. \tag{10}$$

Problem 3 (generalized Rastrigin function ($D = 30$)).

$$f(x) = \sum_{i=1}^{D} \left[x_i^2 - 10\cos(2\pi x_i) + 10\right], \quad x_i \in [-5.12, 5.12], i = 1, 2, \cdots, D. \tag{11}$$

Problem 4 (generalized Rosenbrock function ($D = 40$)).

$$f(x) = \sum_{i=1}^{D-1} \left[100\left(x_{i+1} - x_i^2\right)^2 + (x_i - 1)^2\right], \quad x_i \in [-30, 30], i = 1, 2, \cdots, D. \tag{12}$$

Problem 5 (Ackley function ($D = 50$)).

$$f(x) = -20\exp\left(-0.2\sqrt{\frac{1}{D}\sum_{i=1}^{D} x_i^2}\right) - \exp\left(\frac{1}{D}\sum_{i=1}^{D}\cos(2\pi x_i)\right) + 20 + e, \quad x_i \in [-32, 32], \quad i = 1, 2, \cdots, D. \tag{13}$$

For the DE and HDE algorithms, we set $F = 0.5$ and CR = 0.9. The optimization results obtained by three algorithms for these five benchmark problems and the proposed antenna are shown in Table 1. Figure 5 presents the convergence curves of these three algorithms for optimizing the proposed antenna. As shown in Table 1 and Figure 5, the SHDE algorithm has better performance than DE and HDE. Parameter analysis is a common way for selecting the antenna parameters. Here, the parameter analysis is used to obtain an estimated solution, by scanning the six parameters selected in the optimization process one by one. The limitation of parameter analysis is that it cannot handle the interaction effect between variables; thus, compared with the global optimization algorithm, it is less likely to obtain the global optimal solution. Figure 6 presents the reflection coefficients $|S_{11}|$ of the proposed antenna obtained by the parameter analysis and the SHDE algorithm. As shown in the figure, the reflection coefficients of the antenna structure obtained by the parametric analysis violate the design requirements of $|S_{11}| < -10$ dB in the 7.7-8.2 GHz and 11.8-13.2 GHz frequency bands, which are close to the design requirements of $|S_{11}| < -10$ dB at 5.5 GHz and 10.8 GHz. Therefore, the fabrication tolerance may be strictly limited, and the expected performance may not be achieved if the manufacturing deviations occur. After optimized by the SHDE algorithm, the reflection coefficients of the proposed antenna in the frequency range of 3.1-20 GHz are significantly reduced, and better performance is achieved.

Table 1: Fitness results of Problems 1, 2, 3, 4, and 5 and the proposed antenna obtained by DE, HDE, and SHDE.

	DE	HDE	SHDE	Generation
Problem 1	0.049558	0.009214	0.004191	100
Problem 2	0.003316	0.003025	0.002750	10000
Problem 3	32.5006	21.5088	6.964713	10000
Problem 4	14.8919	13.5707	12.9900	3000
Problem 5	0.001441	0.00047	0.00018	2000
This antenna	4.245759	3.895545	3.873154	50

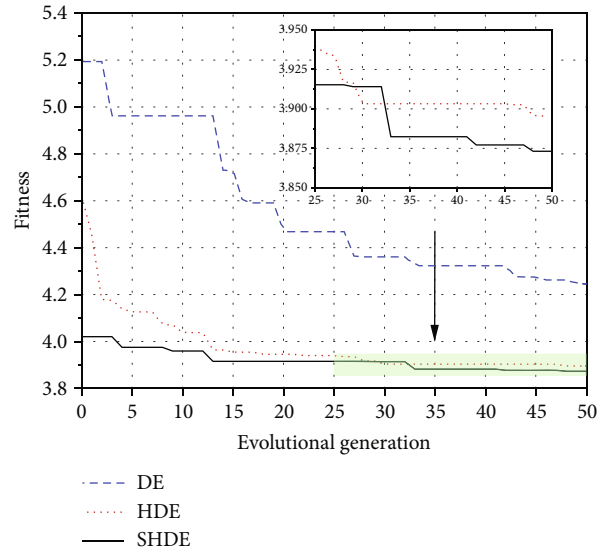

Figure 5: Convergence curves of DE, HDE, and SHDE for optimizing the proposed antenna.

4. Numerical Results and Experimental Verification

The SHDE algorithm is used to optimize the proposed antenna, and the obtained antenna parameter vector is $x^* = (11.8, 19.7, 0.57, 1.2, 2.7, \quad 1.1, 5.1, 8.4, 6.6, 4.8, 5.9, 0.9, 4.6, 13.7, 5.0, 7.5, 3.0, 1.4, 0.7, 4.5, 1.1, 1.0, 1.5, 2.4, 1.8)^T$. The

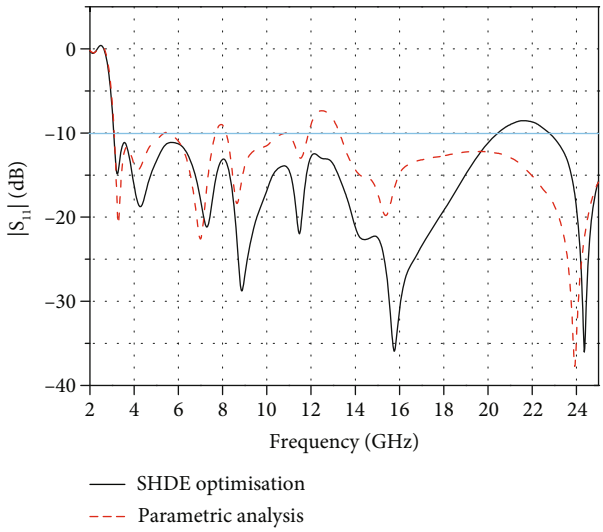

FIGURE 6: Reflection coefficients $|S_{11}|$ of the proposed antenna obtained by the parameter analysis and the SHDE algorithm.

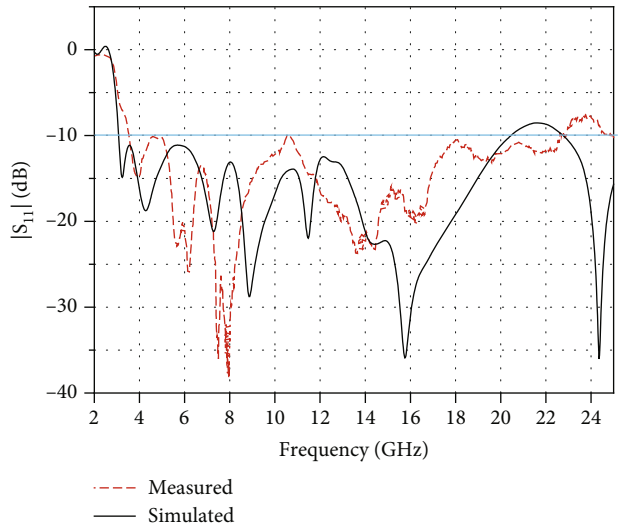

FIGURE 7: Reflection coefficients of the proposed antenna.

overall size of the antenna structure is $11.8 \times 19.7\,\text{mm}^2$, the floor area is only $232.46\,\text{mm}^2$, and the bandwidth of 3.08-20.46 GHz is covered.

The optimized antenna structure has been fabricated and measured. Photographs of the manufactured prototype are shown in Figure 4. The SMA connector is included in the simulation model and the measurement model. Comparison of reflection coefficients of the proposed antenna is shown in Figure 7. The simulation results indicate that the proposed antenna covers the frequency range of 3.08-20.46 GHz with the bandwidth of 147.6%. Comparison between the measurement results and the simulation results shows that the lowest frequency increases from the simulated 3.08 GHz to the measured 3.5 GHz, and at the same time, the highest frequency increases from the simulated 20.46 GHz to the measured 22.6 GHz. Bandwidth of the proposed antenna changes from the simulated 147.6% to the measured 146.4%. Actually, the measured and simulated fluctuation trends are in good agreement, and the expected performance of simulation results has been achieved. The difference between the simulation and the measurement is mainly caused by the manufacturing tolerances and the SMA connector welding imperfections.

Figures 8 and 9 present comparisons of the simulated and measured E-plane (yoz-plane) as well as H-plane (xoz-plane) radiation patterns of the proposed antenna at 6 GHz, 10 GHz, 14 GHz, and 18 GHz. The H-plane characteristics are well aligned. Both the E-plane and the H-plane patterns show good isotropic radiation characteristics. The discrepancies between the measured and simulated E-plane patterns are due to the utilized measurement setup. Further discussion is needed to understand the reason for the poor agreement between the measured and simulated E-plane radiation patterns. In many cases, spurious radiations from the feeding cable and the SMA connector, which are integral parts of the antenna measurement system, have a negative impact on the measurement results in certain orientations. For the small-sized omnidirectional antenna proposed in this paper, the degree of similarity between the radiation pattern and the circle is the main consideration. Due to the low gain of the antenna in each direction, even weak stray radiations in the cable still have a large influence on the measured radiation patterns. This is likely the primary reason for the discrepancy between the measured and simulated E-plane radiation patterns.

Figure 10 presents simulated and measured gains of the proposed antenna in the single direction of $\theta = 0^\circ$ and its simulated peak gains over all directions. As shown in the figure, simulated gains of the proposed antenna in the $\theta = 0^\circ$ direction are rather flat from 3 to 14 GHz. Its simulated gains in the $\theta = 0^\circ$ direction drop below 0 dB after crossing 14 GHz, rapidly recover after reaching the lowest point at 17 GHz, and rise back to above 0 dB at 19 GHz. The measurement and simulation variation trends are basically consistent. The gain decrease in the $\theta = 0^\circ$ direction is mainly due to the shift of the maximum radiation direction when the frequency increases. The peak gains are kept above 2 dB in the whole frequency band, and as the frequency increases, the overall trend is to gradually increase, reaching a maximum of 6 dB. Considering the miniaturized size and extremely wide impedance bandwidth, the gain results are satisfactory. Figure 11 presents simulated and measured radiation efficiencies of the proposed antenna. As shown in the figure, the simulated radiation efficiencies are greater than 80% in the 3-20 GHz band. However, the measured radiation efficiencies are lower than 60% in the 4-12 GHz band and only gradually match the simulated results as the frequency increases. The poor agreement between the measured and simulated radiation efficiencies in the 5-11 GHz band may be attributed to the manufacturing errors and the influence of measurement environment.

The proposed antenna has been compared with some other similar designs in size and bandwidth [1–3, 5–9, 11, 14, 15], as shown in Table 2. Obviously, the antenna structure proposed in this paper is relatively small and covers the largest bandwidth, which is a compromise between size and bandwidth.

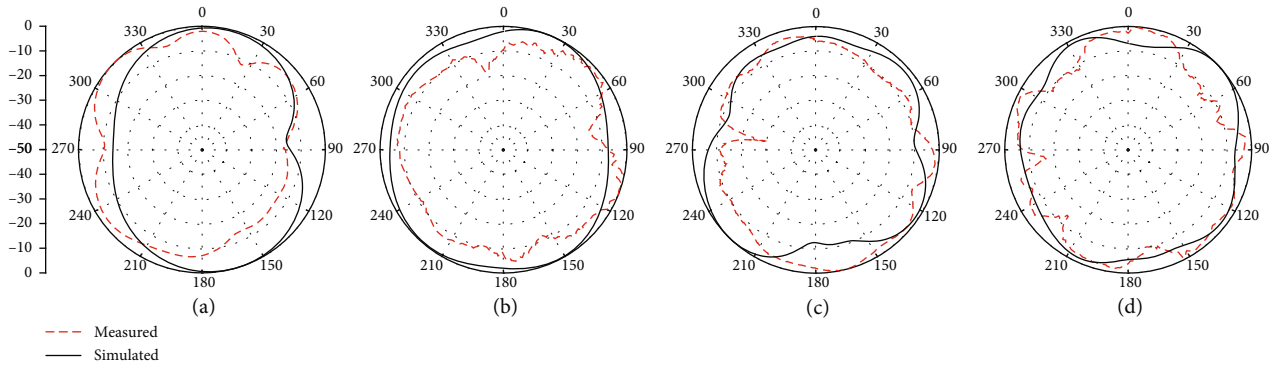

FIGURE 8: Simulated and measured E-plane radiation patterns of the proposed antenna: (a) 6 GHz; (b) 10 GHz; (c) 14 GHz; (d) 18 GHz.

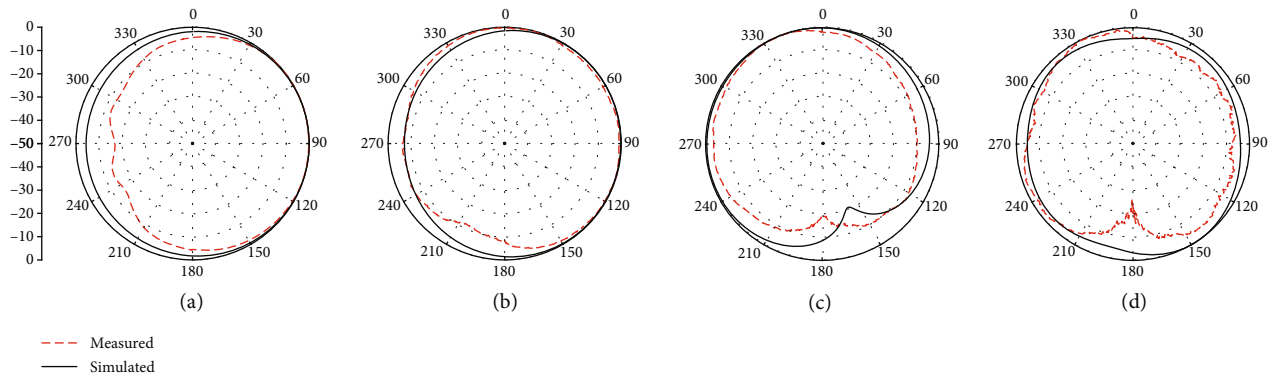

FIGURE 9: Simulated and measured H-plane radiation patterns of the proposed antenna: (a) 6 GHz; (b) 10 GHz; (c) 14 GHz; (d) 18 GHz.

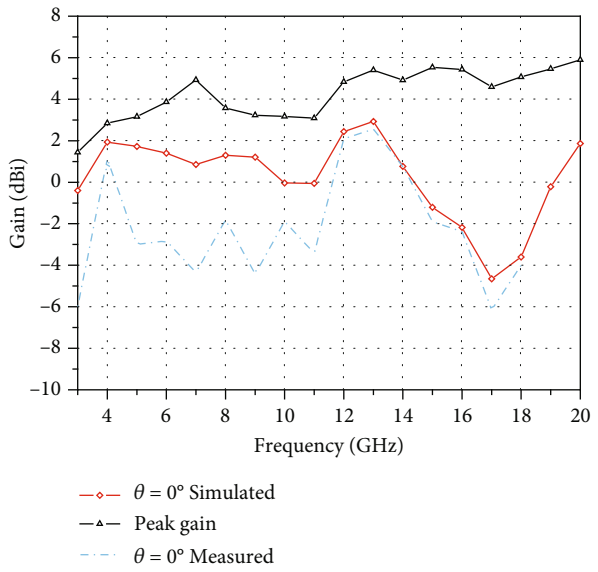

FIGURE 10: Simulated and measured gains of the proposed antenna in the $\theta = 0^\circ$ direction and its simulated peak gains over all directions.

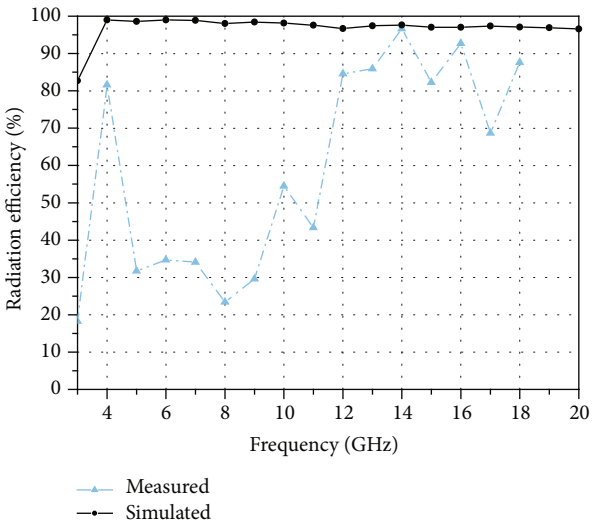

FIGURE 11: Simulated and measured radiation efficiencies of the proposed antenna.

Table 2: Comparison of the proposed antennas with some existing wideband printed antennas in the literatures.

Refs.	Dimensions (mm × mm)	Size (mm^2)	Effective ($\lambda_g \times \lambda_g$)	Footprint (λ_g^2)	Frequency range (GHz)	Bandwidth (%)
[1]	15.8 × 22.0	347.60	0.16 × 0.23	0.037	3.10-10.60	110
[5]	30.0 × 26.0	780.00	0.30 × 0.26	0.078	2.96-19.43	147
[2]	25.0 × 25.0	625.00	0.22 × 0.22	0.049	2.60-13.04	134
[6]	28.0 × 20.0	560.00	0.27 × 0.19	0.051	2.85-11.85	122
[3]	9.45 × 18.5	174.825	0.10 × 0.19	0.019	3.10-12.00	122
[7]	26.0 × 25.0	650.00	0.28 × 0.27	0.076	3.20-12.00	116
[8]	22.0 × 25.0	550.00	0.20 × 0.23	0.046	2.70-10.70	119
[11]	31.0 × 51.5	1596.50	0.26 × 0.43	0.112	2.52-12.91	135
[9]	28.5 × 10.0	285.00	0.29 × 0.10	0.029	3.10-12.00	118
[31]	30.0 × 24.0	720.00	0.35 × 0.28	0.098	3.52-21.00	143
This work	11.8 × 19.7	232.46	0.12 × 0.20	0.024	3.08-20.46	147.6

5. Conclusion

In this paper, a novel ultra-broadband-modified fork-shaped printed antenna is proposed. By using the SHDE algorithm, the proposed antenna can achieve excellent performance in an obviously shorter optimization time. The final antenna structure only with an area of 232.46 mm^2 covers the operating frequency range 3.08-20.46 GHz. The proposed antenna not only covers the UWB frequency band under the premise of ensuring small size but also extends the frequency band to the X and Ku bands to achieve better performance to meet wider communication needs. The measured results are in good agreement with the simulated ones. A comparative study shows that the proposed structure offers better miniaturization rates than some state-of-the-art designs in the literatures, while maintaining acceptable electrical performance. How to improve optimization efficiency of the SHDE algorithm, make it adapt multiobjective optimization, and strengthen the combination of antenna structure design and optimization algorithms remains to be studied further.

Data Availability

Data is available on request.

Conflicts of Interest

The authors declare that they have no conflicts of interest.

Acknowledgments

This work was supported in part by the Hangzhou Institute of Technology of Xidian University (GNYZ2023XJ0407) and Fundamental Research Funds for the Central Universities (QTZX22155 and XJSJ23013).

References

[1] A. Bekasiewicz and S. Koziel, "Structure and computationally efficient simulation-driven design of compact UWB monopole antenna," *IEEE Antennas and Wireless Propagation Letters*, vol. 14, pp. 1282–1285, 2015.

[2] A. K. Gautam, S. Yadav, and B. K. Kanaujia, "A CPW-fed compact UWB microstrip antenna," *IEEE Antennas and Wireless Propagation Letters*, vol. 12, pp. 151–154, 2013.

[3] A. Bekasiewicz and S. Koziel, "Compact UWB monopole antenna for Internet of Things applications," *Electronics Letters*, vol. 52, no. 7, pp. 492–494, 2016.

[4] M. G. N. Alsath and M. Kanagasabai, "Compact UWB monopole antenna for automotive communications," *IEEE Transactions on Antennas and Propagation*, vol. 63, no. 9, pp. 4204–4208, 2015.

[5] M. Akbari, M. Koohestani, C. H. Ghobadi, and J. Nourinia, "A new compact planar UWB monopole antenna," *International Journal of RF and Microwave Computer-Aided Engineering*, vol. 21, no. 2, pp. 216–220, 2011.

[6] S. Nikolaou and M. A. B. Abbasi, "Design and development of a compact UWB monopole antenna with easily-controllable return loss," *IEEE Transactions on Antennas and Propagation*, vol. 65, no. 4, pp. 2063–2067, 2017.

[7] N. Ahmad Jan, S. Hassan Kiani, D. Ali Sehrai et al., "Design of a compact monopole antenna for UWB applications," *Computers, Materials and Continua*, vol. 66, no. 1, pp. 35–44, 2021.

[8] Z. P. Zhong, J. J. Liang, M. L. Fan et al., "A compact CPW-fed UWB antenna with quadruple rejected bands," *Microwave and Optical Technology Letters*, vol. 61, no. 12, pp. 2795–2800, 2019.

[9] A. S. Al-zayed and V. A. Shameena, "Coplanar strip fed UWB antenna with a step cut," *International Journal of RF and Microwave Computer-Aided Engineering*, vol. 24, no. 6, pp. 665–672, 2014.

[10] Y. C. Lin and K. J. Hung, "Compact ultrawideband rectangular aperture antenna and band-notched designs," *IEEE Transactions on Antennas and Propagation*, vol. 54, no. 11, pp. 3075–3081, 2006.

[11] R. Kumar, R. Sinha, A. Choubey, and S. K. Mahto, "A compact microstrip feedline printed antenna with perturbed partial ground plane for UWB applications," *International Journal of RF and Microwave Computer-Aided Engineering*, vol. 31, no. 9, p. e22764, 2021.

[12] A. Foudazi, H. R. Hassani, and S. Mohammad ali nezhad, "Small UWB planar monopole antenna with added GPS/

GSM/WLAN bands," *IEEE Transactions on Antennas and Propagation*, vol. 60, no. 6, pp. 2987–2992, 2012.

[13] S. H. Choi, J. K. Park, S. K. Kim, and J. Y. Park, "A new ultra-wideband antenna for UWB applications," *Microwave and Optical Technology Letters*, vol. 40, no. 5, pp. 399–401, 2004.

[14] W. H. Zong, X. M. Yang, S. Li, X. Y. Qu, and X. Y. Wei, "A compact slot antenna configuration for ultrawideband (UWB) terminals and mobile phones," *International Journal of RF and Microwave Computer-Aided Engineering*, vol. 28, no. 8, p. e21400, 2018.

[15] S. K. Mishra, R. K. Gupta, A. Vaidya, and J. Mukherjee, "A compact dual-band fork-shaped monopole antenna for Bluetooth and UWB applications," *IEEE Transactions on Antennas and Propagation*, vol. 10, pp. 627–630, 2011.

[16] M. Naser-Moghadasi, H. Rousta, and B. S. Virdee, "Compact UWB planar monopole antenna," *IEEE Antennas and Wireless Propagation Letters*, vol. 8, pp. 1382–1385, 2009.

[17] Federal Communications Commission, *Revision of Part 15 of the Commission's Rules regarding UWB Transmission Systems*, First Report, FCC, 2002.

[18] K. V. Price, "Differential evolution," in *Handbook of optimization*, pp. 187–214, Springer, Berlin, Heidelberg, 2013.

[19] R. Storn and K. Price, "Differential evolution–a simple and efficient heuristic for global optimization over continuous spaces," *Journal of Global Optimization*, vol. 11, no. 4, pp. 341–359, 1997.

[20] R. Storn, "System design by constraint adaptation and differential evolution," *IEEE Transactions on Evolutionary Computation*, vol. 3, no. 1, pp. 22–34, 1999.

[21] Y. L. Yan, G. Fu, S. X. Gong, X. Chen, and D. C. Li, "Design of a wide-band Yagi-Uda antenna using differential evolution algorithm," *2010 International Symposium on Signals, Systems and Electronics*, vol. 2, pp. 1–4, 2010.

[22] D. G. Kurup, M. Himdi, and A. Rydberg, "Synthesis of uniform amplitude unequally spaced antenna arrays using the differential evolution algorithm," *IEEE Transactions on Antennas and Propagation*, vol. 51, no. 9, pp. 2210–2217, 2003.

[23] W. Wang, S. X. Gong, X. Wang, Y. Guan, and W. Jiang, "Differential evolution algorithm and method of moments for the design of low-RCS antenna," *IEEE Antennas and Wireless Propagation Letters*, vol. 9, pp. 295–298, 2010.

[24] IEEE, "Standard letter designations for radar-frequency bands-redline," in *IEEE Std 521-2019 (Revision of IEEE Std 521-2002)*, pp. 1–22, Redline, 2020.

[25] J. Brest, S. Greiner, B. Boskovic, M. Mernik, and V. Zumer, "Self-adapting control parameters in differential evolution: a comparative study on numerical benchmark problems," *IEEE Transactions on Evolutionary Computation*, vol. 10, no. 6, pp. 646–657, 2006.

[26] Dassault Systèmes, *CST Microwave Studio*, CST Studio Suite, 2008.

[27] L. Zhang, Y. C. Jiao, H. Li, and F. S. Zhang, "Hybrid differential evolution and the simplified quadratic interpolation for global optimization," in *Proceedings of the first ACM/SIGEVO Summit on Genetic and Evolutionary Computation*, pp. 1049–1052, Shanghai, China, 2009.

[28] L. Zhang, Y. C. Jiao, H. Li, and F. S. Zhang, "Antenna optimization by hybrid differential evolution," *International Journal of RF and Microwave Computer-Aided Engineering*, vol. 20, no. 1, pp. 51–55, 2010.

[29] L. Zhang, *Antenna Optimal Design Technology Based on Differential Evolutionary Algorithm, [Ph.D. thesis]*, Xidian University, China, 2011.

[30] L. Zhang, Y. C. Jiao, B. Chen, and F. S. Zhang, "Synthesis of linear aperiodic arrays using a self-adaptive hybrid differential evolution algorithm," *IET Microwaves, Antennas & Propagation*, vol. 5, no. 12, pp. 1524–1528, 2011.

[31] Z. A. Dayo, Q. Cao, Y. Wang, P. Soothar, B. Muneer, and B. S. Chowdhry, "A compact broadband high gain antenna using slotted inverted omega shape ground plane and tuning stub loaded radiator," *Wireless Personal Communications*, vol. 113, no. 1, pp. 499–518, 2020.